Nanoelectronics and Its New Materials – A NEW ERA OF NANOSCIENCE

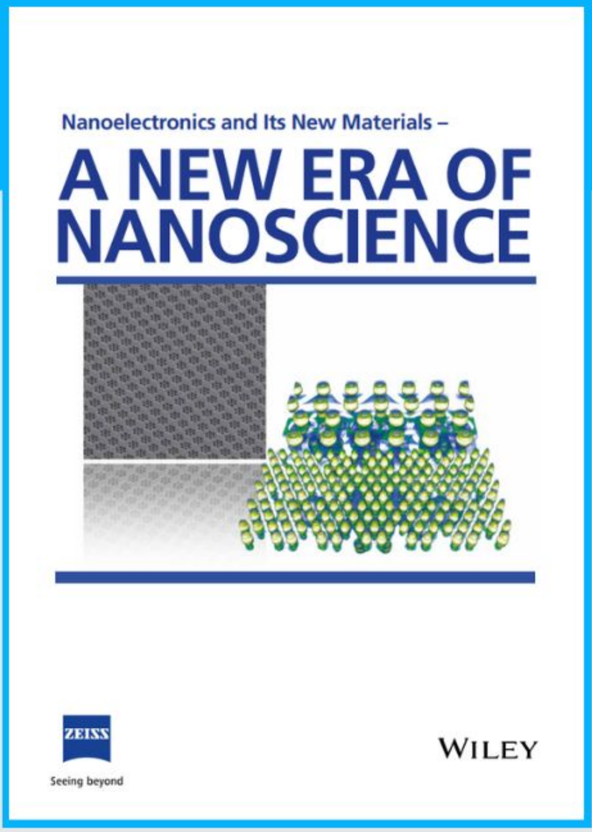

Discover the recent advances in electronics research and fundamental nanoscience.

Nanotechnology has become the driving force behind breakthroughs in engineering, materials science, physics, chemistry, and biological sciences. In this compendium, we delve into a wide range of novel applications that highlight recent advances in electronics research and fundamental nanoscience. From surface analysis and defect detection to tailored optical functionality and transparent nanowire electrodes, this eBook covers key topics that will revolutionize the future of electronics.

To get your hands on this valuable resource and unleash the power of nanotechnology, simply download the eBook now. Stay ahead of the curve and embrace the future of electronics with nanoscience as your guide.

ZEISS

Seeing beyond

WILEY

Heterogeneous Fluorescent Organohydrogel Enables Dynamic Anti-Counterfeiting

Xiaoxia Le, Hui Shang, Shuangshuang Wu, Jiawei Zhang, Mingjie Liu, Yinfei Zheng, and Tao Chen**

Fluorescent patterns showing the unique color change in response to external stimuli are of considerable interest for their applications in anti-counterfeiting. However, there is still a lack of intelligent fluorescent patterns with high-security levels, presenting a dynamic display of encrypted information. In this study, a fluorescent organohydrogel is fabricated through a two-step interpenetrating technique, leading to the co-existence of naphthalimide moieties (DEAN, green-yellow fluorescent monomer) contained Poly(N,N-dimethylacrylamide) (PDMA) hydrogel network and Polyoctadecyl methacrylate (PSMA) organogel network bearing spiropyran moieties (SPMA, photochromic monomer). Due to the unique heterogeneous networks, the fluorescence color goes through a continuous change from green to yellow to red via the fluorescence resonance energy transfer (FRET) process with the extension of irradiation time. In addition, when H^+ is introduced into the system, SP units exhibit transformation into the protonated merocyanine (MCH^+) rather than merocyanine (MC) under UV light, which inhibits the FRET process. By selectively being treated with H^+, the fluorescent organohydrogel can act as an effective platform for encrypting secret information, making them more difficult to forge.

1. Introduction

Counterfeiting is a global and unignorable problem that poses a severe threat to human health, social economy and even country security.[1] Over the past decades, new anti-counterfeiting materials and corresponding encryption/decryption technologies, including holograms,[2] watermarks,[3] security codes,[4] and fluorescent patterns,[5] have achieved unprecedented development against counterfeiting. Among these available anti-counterfeiting techniques, fluorescent patterns have gained much attention due to their vivid color and ease of color manipulation.[6] So far, various advancements mainly focus on designing and synthesizing novel emitting sources, including carbon dots,[7] lanthanide complexes,[8] upconversion nanoparticles,[9] and organic dyes,[10] for enriching the variety of fluorescent colors from multiple colors to entire colors. Furthermore, much effort has been devoted to develop new fluorescent anti-counterfeiting modes such as the combination of structural color and fluorescent color[11] or adoption of "dual/multichannel" stimulus-response mode[12] for enhancing the anti-counterfeiting level. Nevertheless, the stored information based on the above materials is still facing the risk of being duplicated or counterfeited due to their static fluorescence color outputs, which can be imitated by other alternatives showing the same color.

Stimuli-responsive fluorescent patterns exhibit a dynamic color change in response to external stimuli, including heat, irradiation, mechanical force, and electromagnetic field. These fluorescent patterns show dynamic color change over time after exposure to light and present a vibrant display of encrypted information thus possessing much higher security level due to the increase of anti-counterfeiting dimension.[13] For example, Jiang et al.[14] presented a supramolecular network with the capability of dynamic wrinkle morphology and changeable fluorescence color in response to visible light and acid gas stimuli, which can act as a high-performance anti-counterfeiting material for information recording, hiding, and reading. Wang and co-workers[15] have designed a stimuli-responsive fluorescent pattern by utilizing combinatory chemistry and oxygen-concentration-dependent responsiveness, making the encrypted information hard to be duplicated. However, these typical stimuli-responsive fluorescent patterns

X. Le, H. Shang, S. Wu, J. Zhang, T. Chen
Key Laboratory of Marine Materials and Related Technologies
Zhejiang Key Laboratory of Marine Materials and Protective Technologies
Ningbo Institute of Material Technology and Engineering
Chinese Academy of Sciences
Ningbo 315201, China
E-mail: tao.chen@nimte.ac.cn

X. Le, M. Liu
Key Laboratory of Bioinspired Smart Interfacial Science and Technology of Ministry of Education
School of Chemistry
Beihang University
Beijing 100191, China
E-mail: liumj@buaa.edu.cn

Y. Zheng
Research Center for Intelligent Sensing
Zhejiang Lab
No.1818 West Wenyi Road, Yuhang District, Hangzhou 311100, China

Y. Zheng
College of Biomedical Engineering and Instrument Science
Zhejiang University
Hangzhou 310027, China

Y. Zheng
Key Laboratory for Biomedical Engineering of Ministry of Education
Ministry of China
Zhejiang University
Hangzhou 310027, China

The ORCID identification number(s) for the author(s) of this article can be found under https://doi.org/10.1002/adfm.202108365.

DOI: 10.1002/adfm.202108365

vary fluorescence color via the integration of two or more stimuli-responsive mechanisms, and it is still challenging to fabricate intelligent fluorescent patterns with continuous color change under one single stimulus.

Materials exhibiting time-dependent dynamic fluorescence color show great potential for advanced anti-counterfeiting, in which time is a key for encryption/decryption.[16] For instance, Tian et al.[17] reported a series of polymer/nanoclay nanocomposites with room-temperature phosphorescence (RTP) performance, which can store transient information based on the programmable retention times of the RTP signals by tuning the ratio of polymer and nanoclay. In our previous work, a urease-containing fluorescent hydrogel was fabricated and used to store transient information via tuning the time dimension for an enzyme-catalyzed reaction.[18] These elegant attempts prove that it's possible to control time dimension to realized continuously dynamic fluorescent anti-counterfeiting.

Spiropyrane (SP) and its derivatives have aroused great attention due to their unique photoinduced fluorochromic property. In exposure to wavelengths shorter than 400 nm, spiropyrane convert to merocyanine (MC) form.[19] Dynamic polychromatic fluorescence can be realized via time-gated UV irradiation by combining the SP unit with an appropriate fluorescent monomer. Herein, a fluorescent organohydrogel p(DMA-DEAN)/p(SMA-SPMA) is fabricated as an anti-counterfeiting material via a two-step interpenetrating technique, presenting dynamic color change based on the FRET process ascribed to the water-induced microphase separation of heterogeneous networks.

As shown in **Scheme 1**, the prepared fluorescent organohydrogel composed of interpenetrating hydrogel and organogel

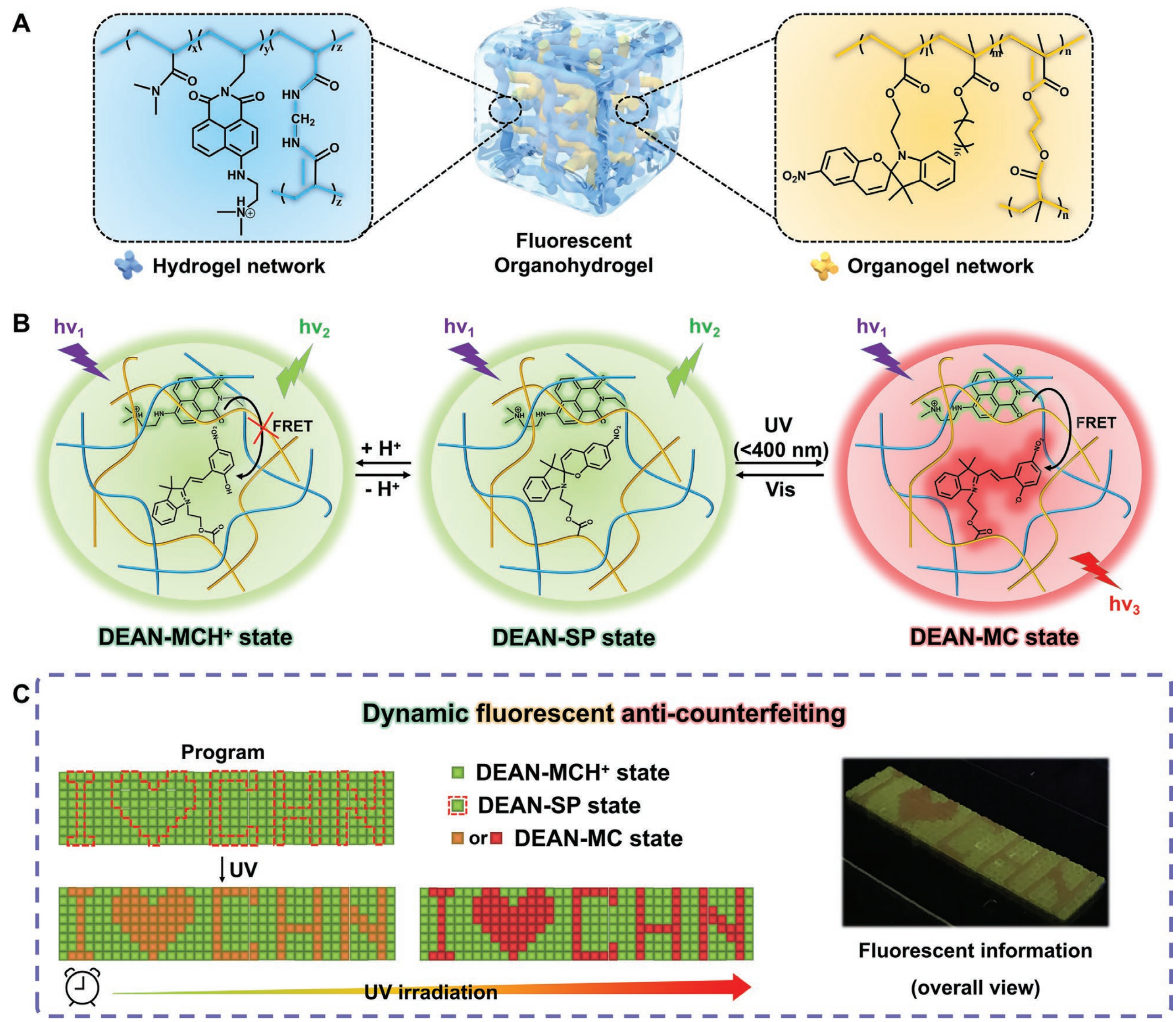

Scheme 1. Schematic illustration of fluorescent organohydrogel p(DMA-DEAN)/p(SMA-SPMA) for dynamic anti-counterfeiting. A) The fluorescent organohydrogel was comprised of fluorescent monomer (DEAN, green) copolymerized DMA in hydrogel network and fluorescent monomer (SPMA, red after UV irradiation) copolymerzied with SMA in organogel network. B) FRET processes between DEAN and SPMA can be triggered by UV (365 nm) without H^+ involved. C) The procedures of encryption and dynamic fluorescent decryption, for example, the encrypted information of "I ♡ CHN" emitting red color finally shows up through UV irradiation.

networks. Containing naphthalimide moieties (DEAN) in the hydrophilic Poly(*N,N*-dimethylacrylamide) (PDMA) block, the hydrogel network emits green-yellow fluorescence under UV light. In contrast, the organogel network bearing spiropyran moieties (SPMA) in the hydrophobic Polyoctadecyl methacrylate (PSMA) block exhibits on-off switching of red fluorescence emission via being exposed to UV light (<400 nm) or visible light, respectively. Due to the special heterostructure of this system, the FRET process can occur between DEAN units (light-absorbing donor) and opened merocyanine units (MCMA, energy-receiving acceptor) when H^+ was not involved (Scheme 1B). Once H^+ interferes with the ring-opening reaction, the structure of SPMA moieties transfers from SP state into MCH^+ state rather than MC state under UV irradiation, inhibiting the FRET process and contributing to the original green-yellow fluorescence instead of red fluorescence. Manipulation of fluorescence color depends on the presence of proton, programmed information can be loaded by selectively treating organohydrogels with a H^+ solution. For example, the encrypted information of "I ♡ CHN" can be loaded by assembling fluorescent organohydrogels in a pixelated array (37×8), at DEAN-SP state and DEAN-MCH^+ state, respectively. The hidden information can be decoded gradually after applying UV light (365 nm) based on the FRET process, showing a dynamic fluorescent color change from green to yellow and finally red with the extension of irradiation time (Scheme 1C).

2. Results and Discussion

2.1. The Fabrication and Characterization of Heterogeneous Organohydrogels

The method of preparing heteronetwork organohydrogels was according to previous work.[20] Briefly, the hydrogel network was firstly fabricated by co-polymerization of N,N-dimethylacrylamide (DMA), and 4-(N, N-dimethylaminoethylene)amino-N-allyl-1,8 naphthalimide (DEAN) (Scheme S1 and Figure S1, Supporting Information) in the presence of N,N′-methylene bis(acrylamide) (BIS) as a crosslinker and ammonium persulfate (APS) as an initiator. After dehydrating in acetone, the gel was immersed in an ethanol solution containing hydrophobic monomer stearyl methylacrylate (SMA), photochromic spiropyran-based monomer (SPMA) (Scheme S2 and Figure S2, Supporting Information), Ethylene dimethacrylate (EGDMA) as a crosslinker and 2,2-Diethoxyacetophenone (DEAP) as a photoinitiator. By in situ polymerization of the oleophilic polymer network, p(DMA-DEAN)/p(SMA-SPMA) organohydrogel within interpenetrating heteronetworks can be obtained after removing unreacted monomers in ethanol. Then solvent displacement was carried out in the water (Figure S6, Supporting Information). Both ^{1}H NMR spectra of p(DMA-DEAN) hydrogel and p(DMA-DEAN)/p(SMA-SPMA) organohydrogel were shown in Figures S7 and S8 (Supporting Information), and the latter shows the typical signal of -C-C-H at the range of 0.9–1.5 ppm, which belonging to long pSMA alkane chains.

As shown in **Figure 1**A, the initial organohydrogel emits green-yellow fluorescence under UV light (365 nm) due to DEAN moieties in the hydrophilic network. The morphologies of the organohydrogel were firstly analyzed by Scanning Electron Microscope (SEM). As can be seen in Figure 1B, the hydrophobic network turns into spheres. And it clings to hydrophilic network, leading to a uniform structure, which may ascribe to the microphase separation triggered by the solvent exchange in water. This kind of heterostructural network is the key to ensure the unique fluorescent properties of the organohydrogel for the following two reasons: 1) First of all, the bi-continuous oleogel network and hydrogel network make it possible for the coexistence of both hydrophobic and hydrophilic fluorescent monomers in one bulk material without considering fluorescence quenching caused by aggregation. 2) More importantly, the effective FRET channels between DEAN and SPMA were established by the hydrophobic microzones, which were formed via water-induced microphase separation after the as-prepared organohydrogel being soaked in H_2O.

Given the coexistence of organogel network and hydrogel network is the prerequisite for guaranteeing the dynamic fluorescence, the first step is to make sure the successful introduction of organogel network and fluorescent monomer SPMA. Compared to the pure p(DMA-DEAN) hydrogel with a contact angle (CA) of 56.3°, p(DMA-DEAN)/p(SMA-SPMA) organohydrogel shows an increase in CA to about 88.6° due to the integration of organogel network (Figure 1B), which indicates the successful introduction of the hydrophobic network. The chemical composition and structure of both p(DMA-DEAN) hydrogel and p(DMA-DEAN)/p(SMA-SPMA) organohydrogel were measured by attenuated total reflection Fourier transformed infrared spectrometer (ATR-FTIR). As shown in Figure 1C (red line), the p(DMA-DEAN)/p(SMA-SPMA) organohydrogel shows characteristic peaks at 2917.7 and 2845.6 cm^{-1}, which are attributable to the stretching vibrations of the C-H bond attached to alkane chains of SMA. Besides, compared to p(DMA-DEAN) hydrogel (black line), the newly emerging peak located at 1725.2 cm^{-1} corresponds to the stretching vibrations of C=O bond belonging to ester group of SMA. Owning long alkane chain, octadecyl methacrylate is easy to crystalize and form hydrophobic domains, especially when the heterogeneous networks are filled with water. The X-ray diffraction patterns of p(DMA-DEAN) hydrogel and p(DMA-DEAN)/p(SMA-SPMA) organohydrogel are shown in Figure 1D. In contrast, the former displays a remarkable broad peak while the later shows two narrow and separated peaks, indicating the formation of discrete crystalline domains. Furthermore, the differences between p(DMA-DEAN) hydrogel and p(DMA-DEAN)/p(SMA-SPMA) organohydrogel can also be reflected in their thermomechanical characteristics. In contrast, p(DMA-DEAN) hydrogel firstly decreased in *G*' and then maintained an almost constant *G*' when temperature increased from 25 to 80 °C, the organohydrogel exhibited two-step and sharp descent, which can be attributed to the first melting process of PSMA crystalline domains (T_m = 35 °C)[21] and followed by the procedure of breaking the hydrogen bonds in hydrogel network (Figure 1E). Meanwhile, through dynamic mechanical analysis (DMA), the introduction of hydrophobic polymeric network can endow the organohydrogel with another two melting peaks when compared with pure p(DMA-DEAN) hydrogel (Figure 1F). The new arising melting peaks are ascribed to the hydrophobic crystalline regions with varying sizes, which were composed of PSMA chains with different lengths. When fluorescent monomer DEAN (green-yellow) was introduced into the hydrogel network and photochromic fluorescent monomer SPMA (red, after UV irradiation) was brought into organogel network, confocal laser scanning microscopy

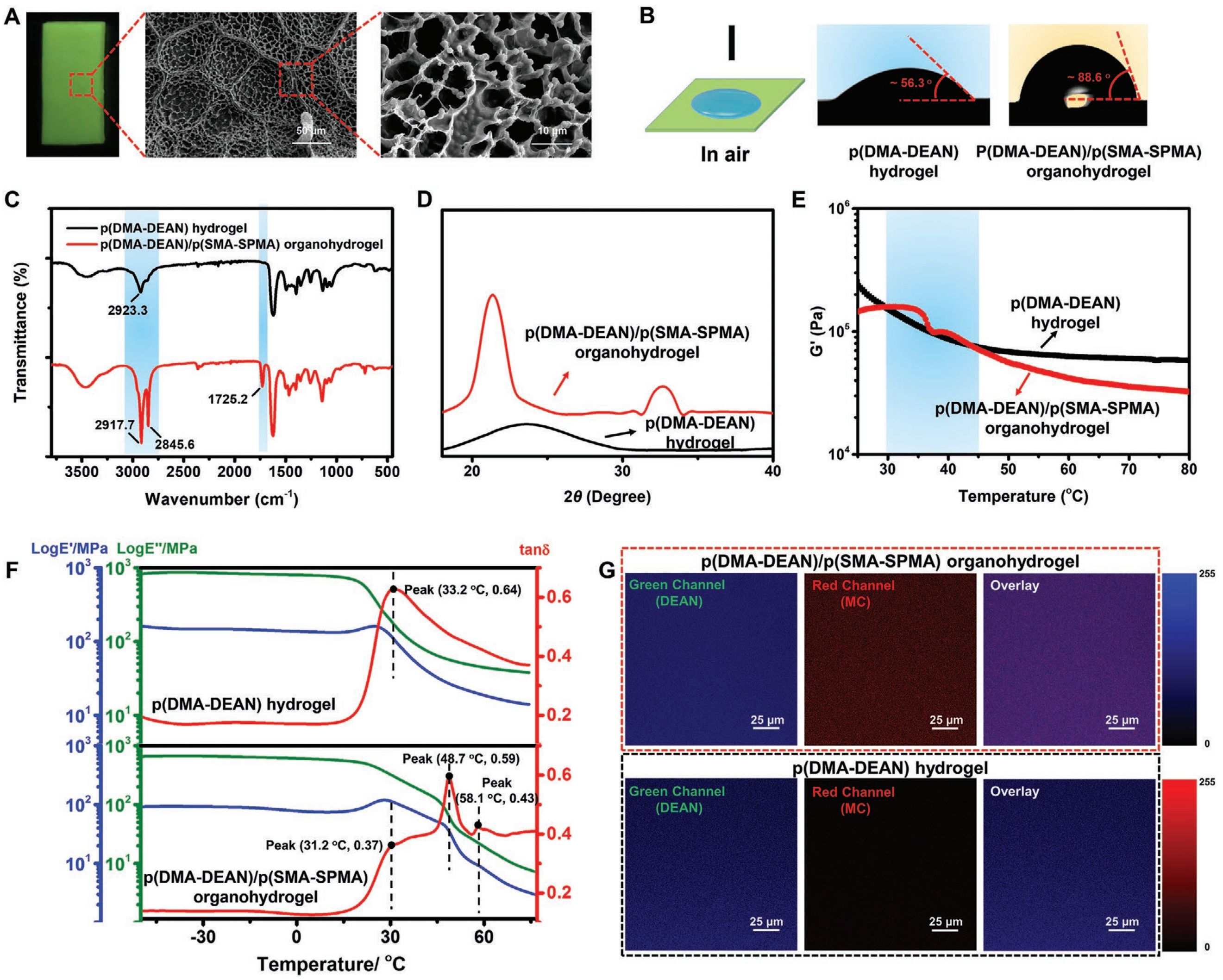

Figure 1. Characterization of p(DMA-DEAN)/p(SMA-SPMA) organohydrogel and p(DMA-DEAN) hydrogel. A) Photograph and cross-section SEM images of p(DMA-DEAN)/p(SMA-SPMA) organohydrogel. Photo was taken under UV light (365 nm). Comparison of contact angles B), FT-IR spectra C), X-ray diffraction patterns D), G' in the range of 25 to 80 °C at a constant shear strain of 1% and frequency of 1 rad s^{-1} E), Dynamic mechanical analysis (DMA) F) of pure p(DMA-DEAN) hydrogel and p(DMA-DEAN)/p(SMA-SPMA) organohydrogel. G) CLSM images of p(DMA-DEAN)/p(SMA-SPMA) organohydrogel and pure p(DMA-DEAN) hydrogel, including Green Channel for DEAN, Red Channel for MCMA and Overlay. The scale bar is 25 µm.

(CLSM) was used to characterize both organohydrogel and PDMA hydrogel. The successful and uniform insertion of fluorescent monomer SPMA and formation of organogel network results the red channel lighting up (Figure 1G). All above results proved the successful formation of heterogeneous polymeric network.

2.2. Dynamic Fluorescent Behavior of Organohydrogels

In this fluorescent organohydrogel system, the naphthalimide moieties emit green-yellow fluorescence. In contrast, the photochromic spiropyran moieties can transform between closed form (colorless) and ring-opened form (red fluorescence) by switching the irradiation of UV and visible light (Figures S3–S5, Supporting Information). Interestingly, our organohydrogel shows dynamic fluorescence change from original green to yellow and finally red with the extension of UV irradiation time. As illustrated in **Figure 2**A, a strawberry-shaped organohydrogel goes through a "ripening" process in about 8 min with the color change from green to yellow and red, which is due to the FRET process (Movie S1, Supporting Information).

To elucidate the mechanism of dynamic fluorescence change, theoretical simulation and experimental measurements have been conducted. As shown in Figure 2B, the UV–vis absorption spectrum of DEAN has a characteristic absorption band at the range of 380–480 nm (λ_{max} = 440 nm), under which the DEAN emits green fluorescence (λ_{ex} = 440 nm) with the emission peak of 550 nm. Meanwhile, MCMA exhibits a distinct absorption band at the range of 500–600 nm (λ_{max} = 550 nm), which exactly overlaps with the fluorescence emission band (λ_{ex} = 440 nm) of DEAN, indicating the effective FRET channel can be constructed between naphthalimide moiety and MCMA unit.[22] To test this hypothesis, density functional theory (DFT) calculations were first employed to analyze the energy gaps and orbital energy

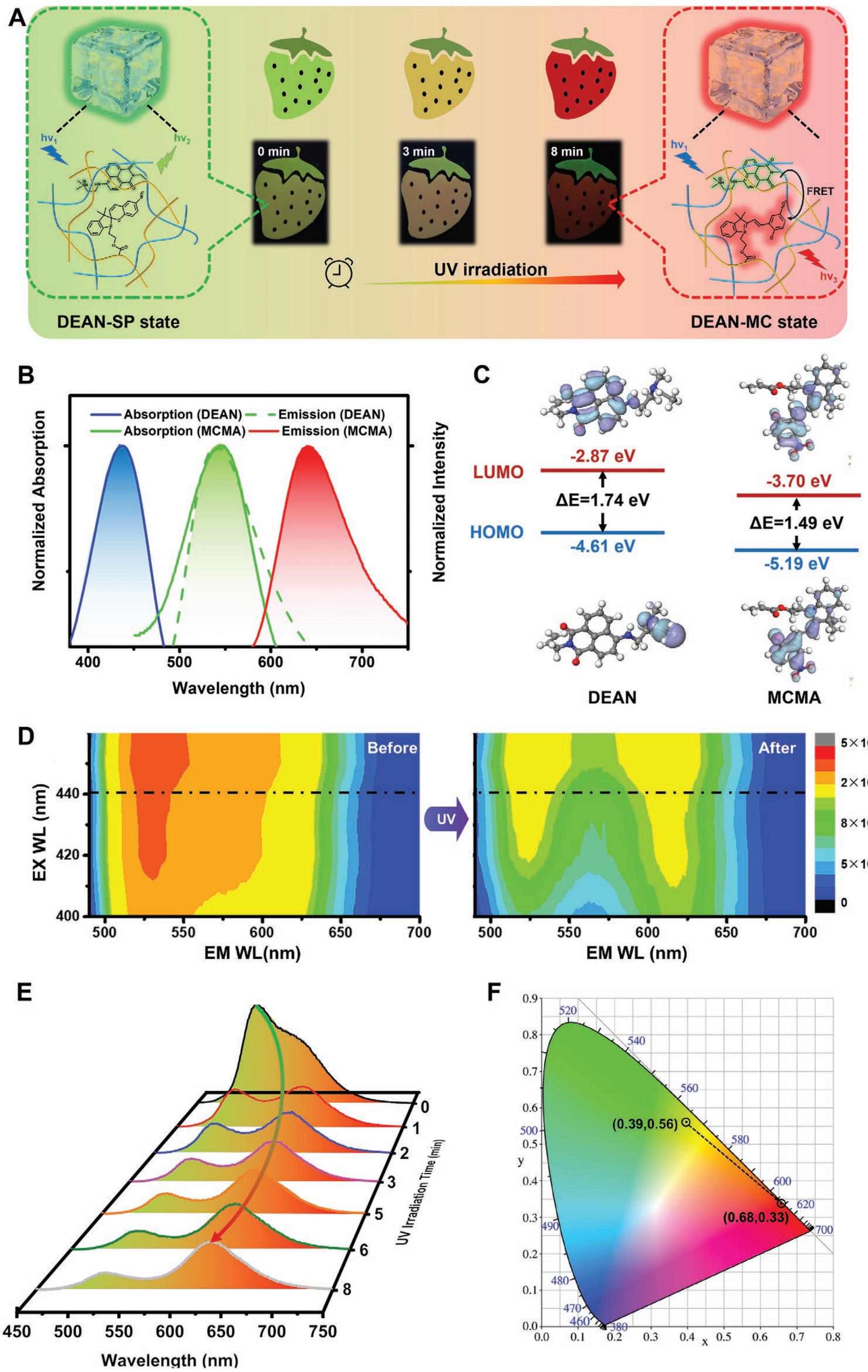

Figure 2. Realization of dynamic fluorescent change. A) Illustration of the mechanism of fluorescence changes and images of strawberry-shaped p(DMA-DEAN)/p(SMA-SPMA) organohydrogels upon exposing to 365 nm UV light. B) The normalized absorption spectra and emission spectra of DEAN as well as MCMA, showing a big overlap between the absorption peak of MCMA and the fluorescent emission peak of DEAN. C) The energy of highest occupied molecular orbital (HOMO) and lowest unoccupied molecular orbital (LUMO) of DEAN and MCMA, respectively. D) PL mapping spectra of p(DMA-DEAN)/p(SMA-SPMA) organohydrogel before and after UV irradiation (365 nm). E) Fluorescence spectra of p(DMA-DEAN)/p(SMA-SPMA) organohydrogel (λ_{ex} = 440 nm) upon irradiation of UV light with different time (0, 1, 2, 3, 5, 6, and 8 min). F) Fluorescence color change of p(DMA-DEAN)/p(SMA-SPMA) organohydrogel before and after UV irradiation at a CIE (1931) chromaticity diagram.

levels of the fluorescent monomers involved (Figure 2C and Figure S9: Supporting Information). As individual monomer moieties tend to share a similar energy level on the polymer backbone, we performed the calculations of single fluorescent monomer, including DEAN and MCMA (Figure 2C). Compared with the MCMA (5.19 eV), DEAN (4.61 eV) acts as the donor occupying high position of highest occupied molecular orbital (HOMO), indicating the possibility of electron transfer from naphthalimide moieties to merocyanine moieties.[23] The PL mapping spectrum (Figure 2D) reveals that there is only a green emission center in the p(DMA-DEAN)/p(SMA-SPMA) organohydrogel (left). Relatively, UV light (365 nm) triggered ring-opening process of spiropyran moieties leads the emergence of red emission centers and the weakening of green emission centers in the organohydrogel (right). Under the selective excitation of 440 nm, the 617 nm emission of MCMA was significantly enhanced. In comparison, the fluorescent intensity of DEAN at 527 nm gradually decreased when the exposure time was extended from 0 to 8 min (Figure 2E), which can also be observed through the fluorescent intensity ratios at 617 and 527 nm (I_{617}/I_{527}) (Figure S10, Supporting Information). On turning off the UV light, the red fluorescence of organohydrogel faded to its original green color (Figure S11, Supporting Information), and the cyclic reversible fluorescence emission behavior can be repeated at least ten times via switching between UV and vis light (Figure S12, Supporting Information). The Commission Internationale de L' Eclairage (CIE) coordinates of the fluorescence of p(DMA-DEAN)/p(SMA-SPMA) organohydrogel before and after UV irradiation are (0.39,0.56) and (0.68,0.33), corresponding to green-yellow and red emissions, respectively (Figure 2F). In addition, fluorescence decay curves and fluorescence quantum yields were measured (Figure S13, Supporting Information). Being fitted by a double-exponential function, the average lifetime of the DEAN-SPMA organohyrogel was calculated to be 63.5 ns, which reduced to 60.4 ns after exposing to UV light for 8 min, with a concomitant decrease of the fluorescence quantum yield from 17.5% to 15.2%. All above results are in good agreement with our hypothesis that the occurrence of the FRET process between DEAN moieties and MCMA moieties in the fluorescent organohydrogel.

2.3. The Transformations of Organohydrogels at Different States

It is well known that the spiropyran has three metastable states, including SP, MC, MCH^+ and one unstable state SPH^+, and they can convert to each other in response to certain stimuli such as UV irradiation and H^+ (**Figure 3**A).[24] Specifically, the transformations begin with the cleavage of C_{spiro}—O bond triggered

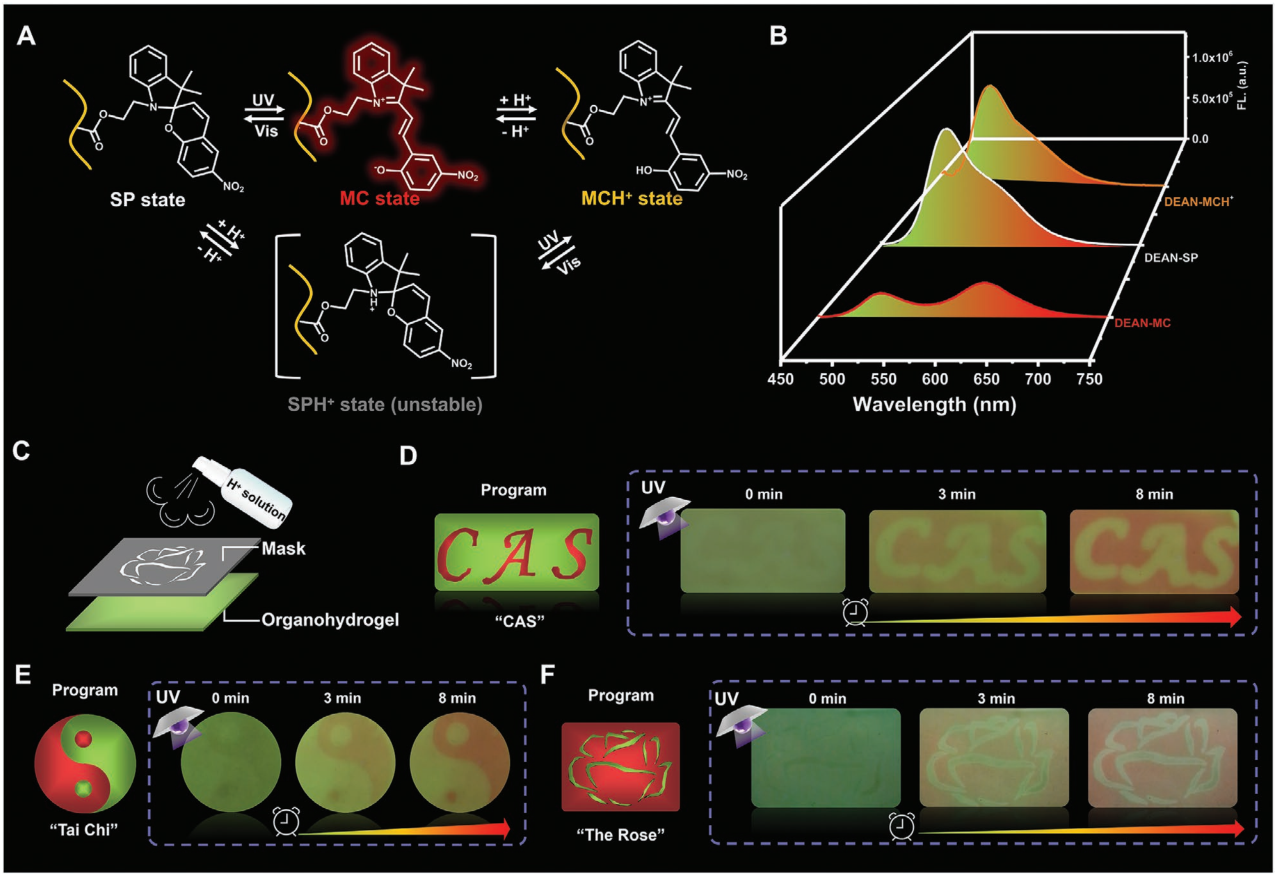

Figure 3. A) Reversible transformations between four states, including spiropyran (SP), merocyanine (MC), protonated merocyanine (MCH^+) and protonated spiropyran (SPH^+). B) Fluorescence spectra of organohydrogel at different states (DEAN-SP, DEAN-MC, and DEAN-MCH^+). C) Schematic illustration of patterning achieved by partially treating a whole piece of organohydrogel with H^+ solution via the assistance of programmed mask. Photos showing dynamic fluorescence decryption of programmed patterns such as D) CAS, E) Tai Chi and F) The Rose on exposing to UV light for 8 min.

by either UV light or H^+, the difference is that the former leads to SP-MC isomerization (red fluorescence) but the later cause SP-MCH$^+$ transition (yellow fluorescence) (Figures S14 and S15, Supporting Information). When these transformations taking place in our organohydrogel system, our materials were endowed with the fascinating dynamic fluorescence phenomenon. To further insight into the fluorescence property, organohydrogels at three different states, including DEAN-SP, DEAN-MC, and DEAN-MCH$^+$, have been investigated using fluorospectro photometer. As shown in Figure 3B, the fluorescence spectra of organohydrogel at DEAN-SP state was almost identical to the one at DEAN-MCH$^+$ state ($\lambda_{ex} = 440$ nm). In comparison, organohydrogel at DEAN-MC state was totally different within a new peak appearing at 617 nm and dramatically reduced emission intensity at 527 nm. Based on this considerable difference in fluorescence color between the two states after UV irradiation, the programmed information can be loaded by treating the organohydrogel with H^+ solution with the assistance of masks (Figure 3C). For example, the pattern of "CAS" was firstly recorded and hidden on the surface of organohydrogel, which can experience a dynamic fluorescence variation (green-yellow-red) under UV irradiation as time goes on (Movie S2, Supporting Information). Analogously, the Chinese "Tai Chi" pattern and pattern "The Rose" in Figure 3E,F both show dynamic decryption process by varying the color of fluorescent emission (Movies S3 and S4, Supporting Information). Once exposed to natural light, all the decrypted pattern will fade away unless UV light is applied again (Figures S16 and S17, Supporting Information).

2.4. Dynamic Information Decryption Based on Fluorescent Organohydrogels

As a proof-of-concept of enhanced anti-counterfeiting level, an encrypted message "2021" was created as schematically depicted in **Figure 4**A. The useful codes were made up of organohydrogels

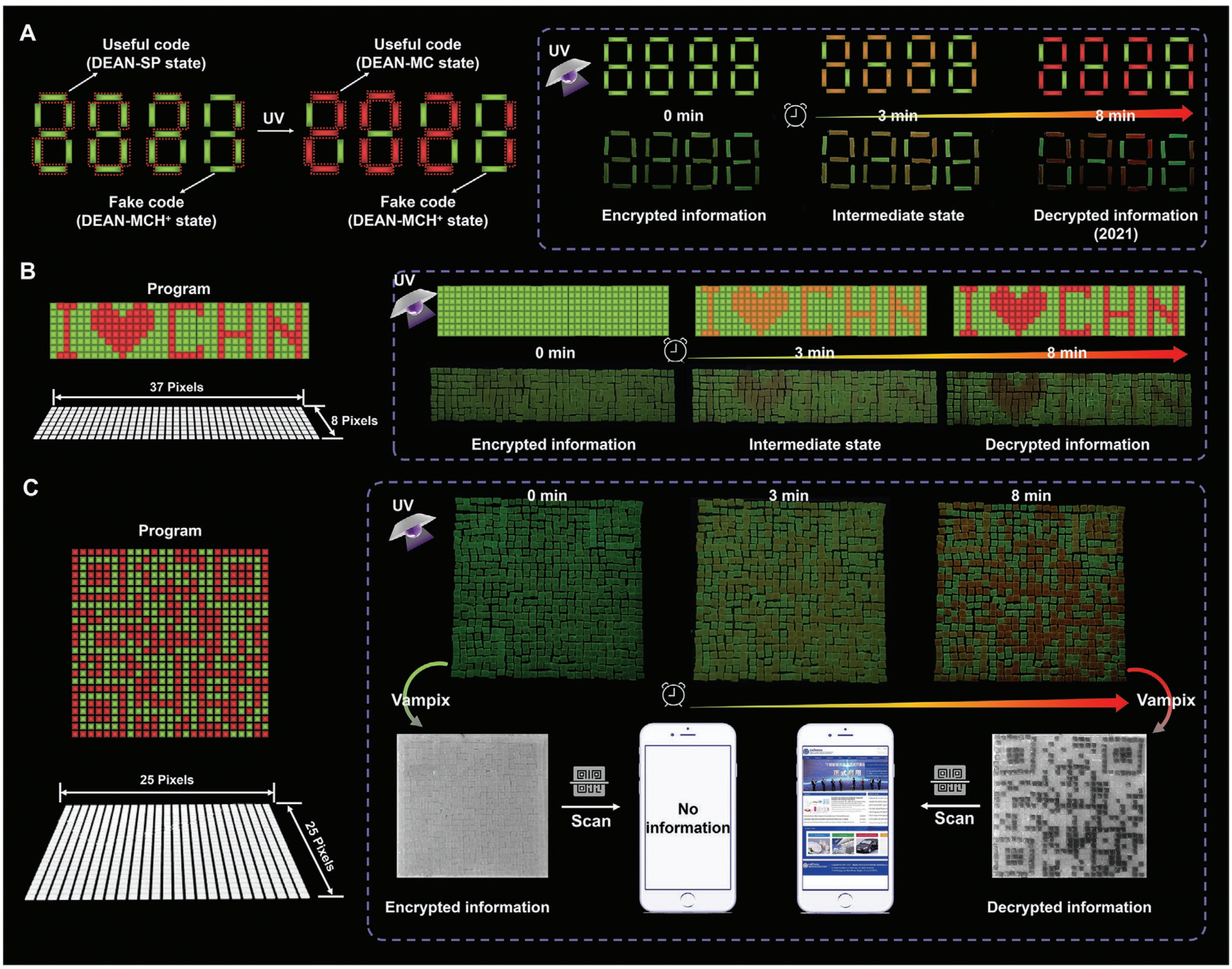

Figure 4. Advanced information encryption and decryption based on fluorescent organohydrogels, exhibiting dynamic fluorescence change. A) The binary codes contain useful code (with red wireframe) and fake code but only the former shows color change upon to UV irradiation, leading to information decryption of "2021". B) The 8×37 "pixelated" array of organohydrogels containing the hidden information of "I ♡ CHN" can be decoded via UV light. C) The QR code made up of organohydrogels in a "pixelated" array (25×25) can be scanned by smartphones only when the decrypted QR code being vampix.

at DEAN-SP state, and organohydrogel constituted the fake codes at DEAN-MCH$^+$ state. Stimulated by UV light, the useful codes underwent fluorescence color changes from green to yellow and red at last. In contrast, the fake codes remained unchanged, corresponding to encrypted information (no data, 0 min), information at intermediated state (yellow "2021", 3 min) and final decrypted information (red "2021", 8 min) (Movie S5, Supporting Information). Then, a "pixelated" array (8×37) of VHB tape was fabricated by assisting of laser cutting machine (each pixel is 2 mm × 2 mm × 0.5 mm) and occupied by the corresponding pixel made up of organohydrogels at DEAN-SP state or DEAN-MCH$^+$ state. The hidden information "I ♡ CHN" can be sequentially decrypted, accompanying by color change from green to yellow and red (Movie S6, Supporting Information). All the decrypted information can be hidden again once exposed to natural light (Figure S18, Supporting Information).

Moreover, a more complicated QR code of different organohydrogels in a "pixelated" array (25×25) was fabricated. Upon UV irradiation, partial green pixels turned into yellow and red, leading to the appearance of a QR code consisting of green and red pixels (Movie S7, Supporting Information). However, the hidden information can still not be scanned directly by a smartphone owing to the low contrast. Finally, the linked website belonging to our institute (http://english.nimte.cas.cn) can be opened after graying the QR code, presenting a much higher level of information encryption.

3. Conclusion

In summary, we presented a fluorescent organohydrogel possessing heterogeneous polymeric networks for dynamic anti-counterfeiting. Consisting of a hydrophilic p(DMA-DEAN) network emitting green-yellow fluorescence and a hydrophobic p(SMA-SPMA) network with photochromic capability, the organohydrogel was obtained by a two-step interpenetrating technology. Owing to the unique heterostructures, the organohydrogel exhibited dynamic fluorescence color change from original green then to yellow and red in response to UV irradiation based on FRET process, which can recover to original state when exposed to Vis light. Except for UV light, the cleavage of C_{spiro}—O bond can also be triggered by H$^+$ and cause SP-MCH$^+$ transition rather than SP-MC isomerization under UV light, inhibiting the FRET process between naphthalimide moieties and merocyanine units and leading to the emittance of green fluorescence. Given the difference of organohydrogel at DEAN-MC state and DEAN-MCH$^+$ state upon to UV light, secret information can be loaded and encrypted by partially treating organohydrogel with H$^+$ solution. Finally, hidden information displayed a dynamic fluorescence variation during the decryption process. In a word, our strategy may provide a new idea for designing and fabricating novel fluorescent anti-counterfeiting materials possessing the capability of dynamic color change, thus improving the security level.

Supporting Information

Supporting Information is available from the Wiley Online Library or from the author.

Acknowledgements

The authors thank Israt Ali from Slovak Academy of Sciences for his kind help with the revision to this manuscript. This work was supported by the National Natural Science Foundation of China (52103246, 51873223, 51773215, 21774138), National Key Research and Development Program of China (2018YFC0114900, 2018YFB1105100), China Postdoctoral Science Foundation (Grant Nos. 2020M671828), the Natural Science Foundation of Ningbo (202003N4361), Youth Innovation Promotion Association of Chinese Academy of Sciences (2017337), Key Research Program of Frontier Science, Chinese Academy of Sciences (QYZDB-SSW-SLH036), the Sino-German Mobility Program (M-0424), and K.C.Wong Education Foundation (GJTD-2019-13).

Conflict of Interest

The authors declare no conflict of interest.

Data Availability Statement

Research data are not shared.

Keywords

dynamic anti-counterfeiting, fluorescent pattern, information decryption, organohydrogel, stimuli responsiveness

Received: August 22, 2021
Revised: September 9, 2021
Published online: September 24, 2021

[1] a) B. Yoon, J. Lee, I. S. Park, S. Jeon, J. Lee, J.-M. Kim, *J. Mater. Chem. C* **2013**, *1*, 2388; b) H. Zhang, D. Hua, C. Huang, S. K. Samal, R. Xiong, F. Sauvage, K. Braeckmans, K. Remaut, S. C. De Smedt, *Adv. Mater.* **2020**, *32*, 1905486.
[2] a) G. Ruffato, R. Rossi, M. Massari, E. Mafakheri, P. Capaldo, F. Romanato, *Sci. Rep.* **2017**, *7*, 18011; b) W. Ye, F. Zeuner, X. Li, B. Reineke, S. He, C. W. Qiu, J. Liu, Y. Wang, S. Zhang, T. Zentgraf, *Nat. Commun.* **2016**, *7*, 11930.
[3] H. Hu, H. Zhong, C. Chen, Q. Chen, *J. Mater. Chem. C* **2014**, *2*, 3695.
[4] P. Kumar, K. Nagpal, B. K. Gupta, *ACS Appl. Mater. Interfaces* **2017**, *9*, 14301.
[5] a) C. Zhang, B. Wang, W. Li, S. Huang, L. Kong, Z. Li, L. Li, *Nat. Commun.* **2017**, *8*, 1138; b) P. She, Y. Ma, Y. Qin, M. Xie, F. Li, S. Liu, W. Huang, Q. Zhao, *Matter* **2019**, *1*, 1644.
[6] a) A. Abdollahi, H. Roghani-Mamaqani, B. Razavi, M. Salami-Kalajahi, *ACS Nano* **2020**, *14*, 14417; b) W. Zhao, Z. Liu, J. Yu, X. Lu, J. W. Y. Lam, J. Sun, Z. He, H. Ma, B. Z. Tang, *Adv. Mater.* **2021**, *33*, 2006844.
[7] a) Z. Tian, D. Li, E. V. Ushakova, V. G. Maslov, D. Zhou, P. Jing, D. Shen, S. Qu, A. L. Rogach, *Adv. Sci.* **2018**, *5*, 1800795; b) C. L. Shen, Q. Lou, C. F. Lv, J. H. Zang, S. N. Qu, L. Dong, C. X. Shan, *Adv. Sci.* **2019**, *6*, 1802331.
[8] a) Z. Li, H. Chen, B. Li, Y. Xie, X. Gong, X. Liu, H. Li, Y. Zhao, *Adv. Sci.* **2019**, *6*, 1901529; b) O. Guillou, C. Daiguebonne, G. Calvez, K. Bernot, *Acc. Chem. Res.* **2016**, *49*, 844.
[9] a) X. Liu, Y. Wang, X. Li, Z. Yi, R. Deng, L. Liang, X. Xie, D. T. B. Loong, S. Song, D. Fan, A. H. All, H. Zhang, L. Huang, X. Liu, *Nat. Commun.* **2017**, *8*, 899; b) W. Ren, G. Lin, C. Clarke, J. Zhou, D. Jin, *Adv. Mater.* **2020**, *32*, 1901430.

[10] a) J. Li, H. K. Bisoyi, S. Lin, J. Guo, Q. Li, *Angew. Chem., Int. Ed.* **2019**, *58*, 16052; b) K. Muthamma, D. Sunil, P. Shetty, *Mater. Today Chem.* **2020**, *18*, 100361.
[11] L. Qin, X. Liu, K. He, G. Yu, H. Yuan, M. Xu, F. Li, Y. Yu, *Nat. Commun.* **2021**, *12*, 699.
[12] Y. Zhao, X. Zhao, M. D. Li, Z. Li, H. Peng, X. Xie, *Angew. Chem., Int. Ed.* **2020**, *59*, 10066.
[13] a) Z. Gao, Y. Han, F. Wang, *Nat. Commun.* **2018**, *9*, 3977; b) W. Tian, J. Zhang, J. Yu, J. Wu, J. Zhang, J. He, F. Wang, *Adv. Funct. Mater.* **2018**, *28*, 1703548; c) J. Du, L. Sheng, Y. Xu, Q. Chen, C. Gu, M. Li, S. X. Zhang, *Adv. Mater.* **2021**, *33*, 2008055.
[14] T. Ma, T. Li, L. Zhou, X. Ma, J. Yin, X. Jiang, *Nat. Commun.* **2020**, *11*, 1811.
[15] L. Ding, X. D. Wang, *J. Am. Chem. Soc.* **2020**, *142*, 13558.
[16] J. Tan, Q. Li, S. Meng, Y. Li, J. Yang, Y. Ye, Z. Tang, S. Qu, X. Ren, *Adv. Mater.* **2021**, *33*, 2006781.
[17] X. Yao, J. Wang, D. Jiao, Z. Huang, O. Mhirsi, F. Lossada, L. Chen, B. Haehnle, A. J. C. Kuehne, X. Ma, H. Tian, A. Walther, *Adv. Mater.* **2021**, *33*, 2005973.
[18] X. Le, H. Shang, H. Yan, J. Zhang, W. Lu, M. Liu, L. Wang, G. Lu, Q. Xue, T. Chen, *Angew. Chem., Int. Ed.* **2021**, *60*, 3640.
[19] R. Klajn, *Chem. Soc. Rev.* **2014**, *43*, 148.
[20] H. Gao, Z. Zhao, Y. Cai, J. Zhou, W. Hua, L. Chen, L. Wang, J. Zhang, D. Han, M. Liu, L. Jiang, *Nat. Commun.* **2017**, *8*, 15911.
[21] S. Zhuo, Z. Zhao, Z. Xie, Y. Hao, Y. Xu, T. Zhao, H. Li, E. Knubben, L. Wen, L. Jiang, M. Liu, *Sci. Adv.* **2020**, *6*, eaax1464.
[22] K. E. Sapsford, L. Berti, I. L. Medintz, *Angew. Chem., Int. Ed.* **2006**, *45*, 4562.
[23] G. Sun, Y. C. Wei, Z. Zhang, J. A. Lin, Z. Y. Liu, W. Chen, J. Su, P. T. Chou, H. Tian, *Angew. Chem., Int. Ed.* **2020**, *59*, 18611.
[24] a) P. K. Kundu, G. L. Olsen, V. Kiss, R. Klajn, *Nat. Commun.* **2014**, *5*, 3588; b) Q. M. Zhang, W. Wang, Y.-Q. Su, E. J. M. Hensen, M. J. Serpe, *Chem. Mater.* **2015**, *28*, 259.